

# Effect of threading defects on InGaN/GaN multiple quantum well light emitting diodes

M. S. Ferdous,<sup>a)</sup> X. Wang, M. N. Fairchild, and S. D. Hersee

Center for High Technology Materials, University of New Mexico, Albuquerque, New Mexico 87106, USA

(Received 24 August 2007; accepted 16 November 2007; published online 5 December 2007)

Photoelectrochemical etching was used to measure the threading defect (TD) density in InGaN multiple quantum well light-emitting diodes (LEDs) fabricated from commercial quality epitaxial wafers. The TD density was measured in the LED active region and then correlated with the previously measured characteristics of these LEDs. It was found that the reverse leakage current increased exponentially with TD density. The temperature dependence of this dislocation-related leakage current was consistent with a hopping mechanism at low reverse-bias voltage and Poole-Frenkel emission at higher reverse-bias voltage. The peak intensity and spectral width of the LED electroluminescence were found to be only weakly dependent on TD density for the measured TD range of  $1 \times 10^7$ – $2 \times 10^8$  cm<sup>-2</sup>. © 2007 American Institute of Physics.

[DOI: 10.1063/1.2822395]

While there is clear evidence that threading defects (TDs) degrade the performance and reliability of GaN-based photonics and electronic devices,<sup>1–4</sup> more information is required concerning the nature of these TD-associated processes. This paper describes ongoing work undertaken to examine the effect of defects on the electrical and optical performance of InGaN/GaN light-emitting diodes (LEDs). The LEDs were fabricated using production quality, blue-emitting InGaN/GaN multiple quantum well (MQW) LED epitaxial wafers from two vendors, which used an epitaxial-layer structure, as shown in Fig. 1. The MQW active region structure in Fig. 1 was similar from both vendors and consisted of four 2 nm thick undoped In<sub>0.15</sub>Ga<sub>0.85</sub>N quantum wells, with 12.5 nm thick undoped GaN barriers. The LED characteristics presented in the subsequent figures combine data from both vendor wafers and no separation of data groups, according to vendor, was observed. This indicated that any minor proprietary modifications to the basic MQW structure had a statistically insignificant effect compared to dominant effect of TD density.

LEDs were fabricated by inductively coupled plasma (ICP) etching a 1 μm deep mesa using etching in argon and chlorine, then e-beam depositing *n*-side Ti/Al/Pt/Au (25/100/50/100 nm) and *p*-side Ni/Au (50/50 nm) Ohmic contacts. The *n* contacts were annealed at 750 °C in N<sub>2</sub> for 15 min and the *p* contacts were annealed in air at 650 °C for 15 min. Ti/Au (50/350 nm) probe pads were also deposited to facilitate on-wafer probe measurements. The typical device size was 340 × 340 μm<sup>2</sup> and four different perimeter-to-area ratios of 58, 88, 126, and 163 cm<sup>-1</sup> were simultaneously fabricated in order to investigate surface perimeter leakage current as described below. The etched mesa sidewall surface was not intentionally passivated in this process. After fabrication, the LEDs were thoroughly characterized and this included measurements of forward and reverse *I*-*V* characteristics and analysis of the electroluminescence spectrum.

The TD density in these LEDs was measured by photoelectrochemical (PEC) etching,<sup>5</sup> which reveals TDs as well-defined “whiskers.” The defect density was accurately determined by counting the number of whiskers within a

known area within the mesa of the LED. Measurement of dislocation density using PEC etching has previously been shown to be entirely consistent with the TD density measured by transmission electron microscopy,<sup>5,6</sup> cathodoluminescence,<sup>7</sup> and photoluminescence.<sup>8,9</sup> The diameter of the PEC etched whiskers was also shown to increase when multiple threading defects agglomerated.<sup>10</sup> PEC etching is only effective for *n*-type GaN as it requires hole accumulation at the semiconductor surface to raise the oxidation state and reactivity of the surface atoms.<sup>11</sup> In this study, we, therefore, ICP etched through the *p* side of the LED structure to expose the *n* side (0.5 μm ICP etch in Fig. 1) of the structure where PEC etching (0.8 μm PEC etch in Fig. 1) was then carried out.

The complete postmeasurement etch process was as follows. The metal contacts were stripped using aqua regia at 60 °C and HF wet etching. The *p* side of the LED was then removed by a 0.5 μm deep ICP etch using standard photolithography. The exposed *n* side of the LED was then subjected to a 0.8 μm PEC etch in order to reveal the threading defects. The TD density was then calculated by scanning electron microscopy (SEM) observation of the number of PEC whiskers in a known plan-view area within the location of the LED mesa, i.e., within the LED region that had previously emitted light. It was assumed that because of the threading nature of the TDs and their orientation along the [0001] crystallographic axis, the TD density measured immediately below the LED active region was representative of the TD density actually inside the LED active region. Figures 2(a) and 2(b) show SEM micrographs of PEC etched, *n*-type

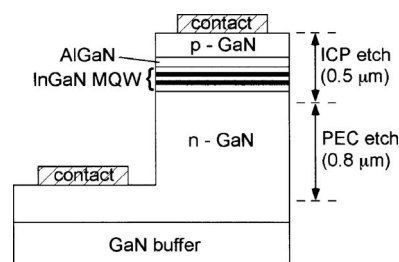


FIG. 1. The MQW InGaN/GaN LED structure. The two primary etches used to reveal the threading dislocations are shown at the right of this figure.

<sup>a)</sup>Electronic mail: ferdous@unm.edu

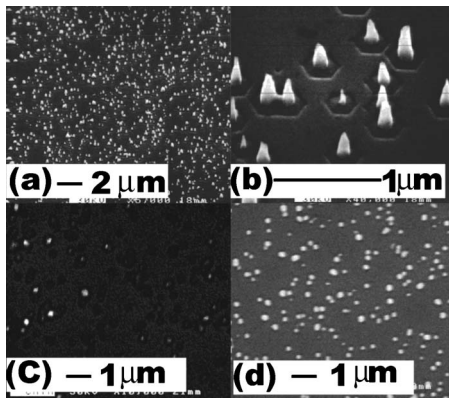


FIG. 2. SEM micrographs of PEC etched *n*-type GaN surfaces of InGaN/GaN MQW LEDs. (a) 45° tilted view with a low magnifications of 5 K. (b) 45° tilted view with a high magnification of 40 K. (c) Plan view with a whisker density of  $1.5 \times 10^7 \text{ cm}^{-2}$  and (d) plan view with a whisker density of  $2 \times 10^8 \text{ cm}^{-2}$ .

GaN surfaces within the LED structure. The whiskers were approximately 250 nm in length, 50–150 nm in diameter, and were oriented along the [0001] crystallographic direction. Figures 2(c) and 2(d) compare plan-view SEM micrographs of PEC etched *n*-type GaN surfaces with whisker densities of  $1.5 \times 10^7$  and  $2 \times 10^8 \text{ cm}^{-2}$ , respectively, which represents the full range of TD density that was measured in these LED wafers.

Figure 3(a) shows the room temperature reverse-biased leakage current density (measured at a reverse voltage of  $-15 \text{ V}$ ) as a function of the average TD density. Each data point is the statistical average of three to eight devices and error bars were drawn at  $\pm 1$  standard deviation with respect to the mean value. The leakage current density increased

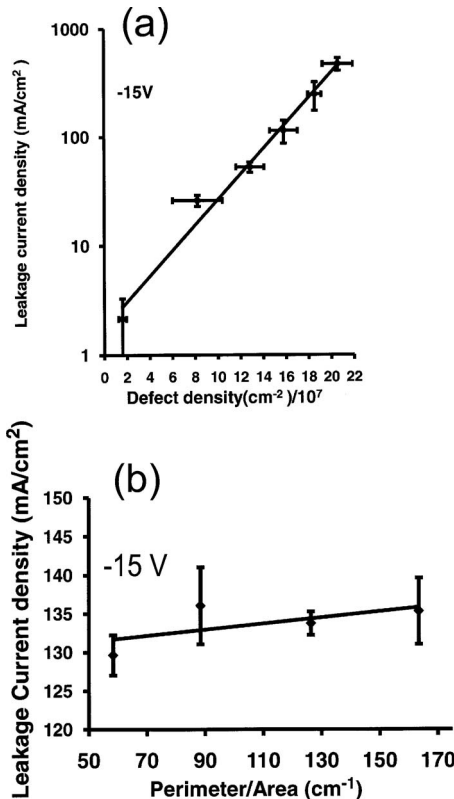


FIG. 3. (a) Reverse leakage current density at  $-15 \text{ V}$  as a function of defect density. (b) Reverse leakage current density at  $-15 \text{ V}$  of different sizes of MQW InGaN/GaN LED, as a function of perimeter/area ratio.

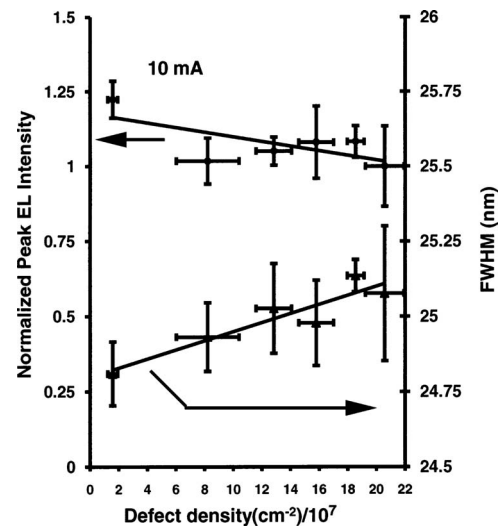


FIG. 4. (Left) Peak electroluminescence intensity at 10 mA as a function of defect density normalized to the lowest peak intensity. (Right) Spectral width (full width at half maximum) as a function of defect density.

exponentially with TD density, growing by 218 times as the TD density increased from  $1.5 \times 10^7$  to  $2 \times 10^8 \text{ cm}^{-2}$ . A superlinear increase of leakage current with defect density was also observed<sup>12</sup> when LEDs were fabricated in the lower defect “wing” regions of an epitaxial laterally overgrown GaN structure. In that case, a 400 times increase in TD density resulted in a 1000 times increase in reverse leakage current.

To verify that the reverse-bias leakage current in these LEDs was a bulk rather than a surface leakage effect, the leakage current density was measured as a function of perimeter-to-area ratio for four different LED sizes [Fig. 3(b)]. The straight line in Fig. 3(b) is a linear least squares fit to the data. The leakage current only increased slightly with perimeter-to-area ratio and from this plot it was calculated that 96.2% of the total leakage current flowed through the LED and only 3.8% of this current was due to surface leakage.

The forward biased light emitting characteristics of these LEDs showed little variation with TD density over the measured TD density range of  $1.5 \times 10^7$  to  $2 \times 10^8 \text{ cm}^{-2}$ . Figure 4 plots the normalized electroluminescence (EL) intensity at 10 mA and full width at half maximum (FWHM) of the EL peak (at 465 nm), as a function of defect density (the EL intensity was normalized to the intensity measured in the sample with the highest TD density). The EL intensity varied by only 22% over the full TD density range. The FWHM of the EL peak varied by only 0.3 nm over this TD range. The forward voltage at the drive current of 10 mA was almost constant (3.5–3.6 V). The variation of the forward-bias *I*-*V* characteristic with TD density at lower currents was not examined and will be the subject of a future study. The insensitivity of forward biased light emission to TDs agrees with the hypothesis that radiative recombination is localized away from TDs, possibly by In-rich regions within the InGaN MQW active region.<sup>1</sup>

The temperature dependence of the reverse-biased leakage current is plotted in Fig. 5 for the temperature range of 295–520 K for LEDs with an area of  $340 \times 340 \mu\text{m}^2$ , and for defect densities of  $1.7 \times 10^8$  and  $5 \times 10^7 \text{ cm}^{-2}$ . The leakage current was found to increase significantly with the reverse voltage and temperature and this variation was well

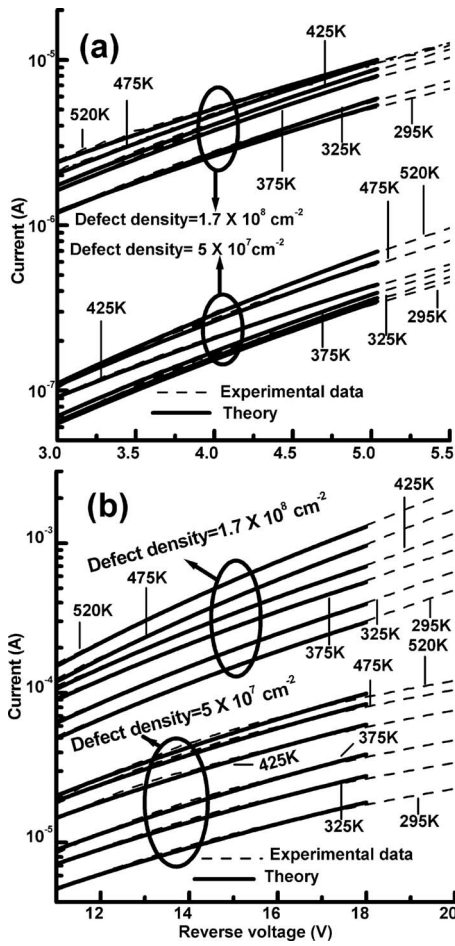


FIG. 5. Experimental and theoretical reverse bias current-voltage characteristics of the LEDs at six different temperatures under (a) low reverse bias and (b) high reverse bias.

modeled using the approach described previously by Kuksenkov *et al.*<sup>13</sup> They found that at low reverse bias the likely conduction mechanism was charged carrier hopping via localized defect-related traps in the depletion region. The low reverse bias hopping mechanism was represented mathematically by

$$I = I(0) \exp \left[ \frac{CeFa}{2KT} \left( \frac{T_0}{T} \right)^{1/4} \right], \quad (1)$$

where the electric field ( $F$ ) in the LED depletion region was calculated using the simplifying assumption that the junction built-in voltage is small compared to the applied reverse bias. The constant  $a$  is assumed to be  $10 \text{ \AA}$  and the constants  $C$  and  $T_0$  were found experimentally<sup>13</sup> to be  $0.4$  and  $1.16 \times 10^{10} \text{ K}$ , respectively. This model is based on Mott's law for variable-range hopping,<sup>14</sup> where current is proportional to the zero bias conductivity  $\sigma(0)$ , which has a temperature dependence given by

$$\sigma(0) \propto \exp \left[ - \left( \frac{T_0}{T} \right)^{1/4} \right]. \quad (2)$$

Figure 5(a) plots Eq. (1) and our experimental data for the reverse-bias voltage range of  $-3$  to  $-5 \text{ V}$ . Assuming that  $a = 10 \text{ \AA}$  as in Ref. 13 the optimized fit to the data yields values for the constants as  $C = 0.4$  and  $T_0 \approx 4.3 \times 10^9 \text{ K}$  for both of the defect densities. The lower value of characteristic temperature ( $T_0$ ) compared to that of Ref. 13 can be attrib-

uted to the reduced bandgap of the InGaN MQW active region in our devices compared to the GaN active region used previously.<sup>13</sup>

At higher reverse bias field-assisted thermal ionization of carriers from the defect-associated traps occurs (the Poole-Frenkel effect) and this increases the leakage current significantly. The leakage current under these conditions was described<sup>13</sup> by

$$I = I_0 \exp \left( \frac{\beta_{PF} F^{1/2}}{kT} \right). \quad (3)$$

Figure 5(b) plots the best fit of Eq. (3) to our experimental data for the reverse-bias voltage range  $-11$  to  $-18 \text{ V}$ . From this fit, we obtain  $\beta_{PF} = 4.9 \times 10^{-4} \text{ eV V}^{-1/2} \text{ cm}^{1/2}$  and  $\beta_{PF} = 3.7 \times 10^{-4} \text{ eV V}^{1/2} \text{ cm}^{1/2}$  for the defect densities of  $1.7 \times 10^8$  and  $5 \times 10^7 \text{ cm}^{-2}$ , respectively. For GaN diodes,<sup>13</sup> it was found to be  $\beta_{PF} = 4.5 \times 10^{-4} \text{ eV V}^{-1/2} \text{ cm}^{1/2}$ .

Figures 5(a) and 5(b) show an excellent fit between the experimentally measured value of leakage current in InGaN MQW LEDs and the theoretically predicted variation of this current with temperature and reverse bias voltage. An excellent fit was also demonstrated for the previously measured GaN LEDs.<sup>13</sup>

In conclusion, the effect of dislocation density measured by PEC etching on the electrical and optical performance of InGaN/GaN MQW LEDs was measured. The reverse-bias leakage current increased exponentially with dislocation density and this leakage current was shown to flow predominantly through the LED active region rather than through the unpassivated LED perimeter surface. The electroluminescence intensity and spectral width appeared to be relatively insensitive to dislocation density. The temperature and bias dependence of this leakage current provides compelling support for the hypothesis<sup>13</sup> that leakage current flows through TDs by carrier hopping between TD defect states. How these defects eventually degrade the forward-biased electroluminescence intensity and lead to device failure is now being studied.

<sup>1</sup>S. Nakamura, *Semicond. Sci. Technol.* **14**, R27 (1999).

<sup>2</sup>D. W. Merfeld, X. A. Cao, S. F. Leboeuf, S. D. Arthur, J. W. Kretchmer, and M. P. D'evelyn, *J. Electron. Mater.* **33**, 1401 (2004).

<sup>3</sup>T. Mukai, K. Takekawa, and S. Nakamura, *Jpn. J. Appl. Phys., Part 2* **37**, L839 (1998).

<sup>4</sup>A. P. Zhang, L. B. Rowland, E. B. Kaminsky, V. Tilak, J. C. Grande, J. Teetsov, A. Vertichikh, and L. F. Eastman, *J. Electron. Mater.* **32**, 388 (2003).

<sup>5</sup>C. Youtsey, L. T. Romano, R. J. Molnar, and I. Adesida, *Appl. Phys. Lett.* **74**, 3537 (1999).

<sup>6</sup>P. Visconti, M. A. Reshchikov, K. M. Jones, D. F. Wang, R. Cingolani, H. Morkoc, R. J. Molnar, and D. J. Smith, *J. Vac. Sci. Technol. B* **19**, 1328 (2001).

<sup>7</sup>C. Diaz-Guerra, J. Piqueras, V. Popa, A. Cojocaru, and I. M. Tiginyanu, *Appl. Phys. Lett.* **86**, 223103 (2005).

<sup>8</sup>A. Watanabe, H. Takahashi, T. Tanaka, H. Ota, K. Chikuma, H. Amano, T. Kashima, R. Nakamura, and I. Akasaki, *Jpn. J. Appl. Phys., Part 2* **38**, L1159 (1999).

<sup>9</sup>L. Macht, J. L. Weyher, A. Grzegorzczak, and P. K. Larsen, *Phys. Rev. B* **71**, 073309 (2005).

<sup>10</sup>M. S. Ferdous, X. Y. Sun, X. Wang, M. N. Fairchild, and S. D. Hersee, *J. Appl. Phys.* **99**, 096105 (2006).

<sup>11</sup>C. Youtsey, G. Bulman, and I. Adesida, *J. Electron. Mater.* **27**, 282 (1998).

<sup>12</sup>P. Kozodoy, J. P. Ibbetson, H. Marchand, P. T. Fini, S. Keller, J. S. Speck, S. P. denBaars, and U. K. Mishra, *Appl. Phys. Lett.* **73**, 975 (1998).

<sup>13</sup>D. V. Kuksenkov, H. Temkin, A. Osinsky, R. Gaska, and M. A. Khan, *Appl. Phys. Lett.* **72**, 1365 (1998).

<sup>14</sup>N. F. Mott, *Philos. Mag.* **19**, 835 (1969).